Prediction of Mode II Delamination Onset Life Under Spectrum Fatigue Loads Using Equivalent Strain Energy Release Rate Concept

A. R. Anilchandra, M. Seshagirachari, Ramesh Bojja, N. Jagannathan and C. M. Manjunatha

Abstract End notched flexure (ENF) test specimens of unidirectional IMA/M21 carbon fiber composite (CFC) were fabricated using standard autoclave process. A Teflon insert was used to simulate a delamination at the midplane. Three-point bend setup tests were conducted at an average frequency of 2 Hz using a 25 kN servo-hydraulic test machine in room temperature conditions. Constant amplitude fatigue tests were done at three different stress ratios, viz. $R = 0.0$, 0.5, and -1.0 to construct the standard G-N_{onset} diagram, similar to S–N curve in its usefulness. N_{onset} was identified as 5% change in initial compliance value. Using an equivalent energy release rate parameter, G_{eq}, all the curves were collapsed into a single curve in the form of Basquin's equation. The equation was subsequently used in predicting the delamination onset-of-growth life under a standard mini-FALSTAFF spectrum load sequence. A fairly good correlation was found between the predicted and experimental mode II onset-of-growth behavior.

Keywords Composite · Delamination · Spectrum load · Onset-of-growth Compliance

Nomenclature

R	Stress ratio
N_{onset}	Number of constant amplitude (CA) fatigue cycles for onset-of-growth
G_{max}	Maximum strain energy release rate (SERR)
G_{min}	Minimum SERR
G_{eq}	Equivalent SERR
G_{IIC}	Critical mode II SERR
G'_{eq}	Basquin's coeffecient
ΔG	Range SERR

A. R. Anilchandra (✉) · M. Seshagirachari · R. Bojja · N. Jagannathan · C. M. Manjunatha
Structural Technologies Division, Fatigue and Structural Integrity Group, CSIR-National Aerospace Laboratories, Bengaluru 560017, India
e-mail: anilchandraar.mech@bmsce.ac.in

R. Prakash et al. (eds.), *Advances in Structural Integrity*,
https://doi.org/10.1007/978-981-10-7197-3_17

γ Best fit parameter
N_b Number of spectrum fatigue load blocks
D Damage fraction

1 Introduction

Aircraft structures are increasingly being replaced with fiber reinforced plastic composites (FRPs) due to their high specific mechanical properties [1]. Delamination in such laminated FRPs possesses a serious threat to the structural integrity since these structures are highly susceptible to in-service-related events such as barely visible impact damages (BVID), assembly and service related events (over tightening, collisions), and so on [2]. While identifying such defects are quite challenging, deciding the fate of such "damaged" structure is also equally challenging [3]. The total life of a delamination under fatigue loading is the sum of number of cycles spent in onset-of-growth (N_{onset}) and subsequently the number of cycles needed for it to propagate to a critical length (N_P). The fatigue loads could be mode I (opening mode), mode II (shearing), mode III (tearing), or a mixed-mode condition. The "no-growth" philosophy of damage tolerant design presumes existence of a delamination owing to the aforementioned reasons and the energy needed in terms of load cycles for it to begin-to-grow, that is, onset-of-growth is regarded as failure of the structure/component [4]. Owing to cost and safety considerations, the aircraft industry would prefer life prediction so that catastrophic failures could be prevented and various prediction models have been proposed in the literature [5].

Life prediction under spectrum fatigue loads can be classified into three major categories, viz., empirical, phenomenological, and physics-based damage models. Empirical models are simple and rely on experimental data (stress levels, stress ratio, or frequency) without considering the inherent damage mechanisms. The Palmgren-Miner (PM) cumulative damage accumulation model is one such life prediction model and was used in our earlier work to predict the onset-of-growth under mode II spectrum loading in a carbon fiber reinforced plastic composite (CFRP) [6]. A novel constant onset life diagram (COLD), similar to constant life diagram (CLD), was proposed and used in the prediction. However, the prediction using CLD involves tedious interpolation technique and this is overcome in the present work by using the equivalent strain energy release rate (G_{eq}) concept. Attempts have been made in the past to normalize stress (S)-number of cycles to failure (N) plot in order to eliminate the effect of specimen geometry and test setup for a particular stress ratio (R) [7]. Petermann and Plumtree [8] used an energy-based approach to merge different R-ratio curves into a single curve and used it in life prediction with a good correlation between the experimental and predicted values. G_{eq} concept, similar to K_{eq} proposed by Hojo et al. [9], was shown to merge various R-ratio curves into a single curve in the G-N_{onset} plot [10].

The aim of the present work is,

- to make use of the G_{eq} concept to merge all the R-ratio curves into a single R-ratio curve in the G-N_{onset} and subsequently use it in predicting the onset-of-growth under mini-FALSTAFF spectrum load sequence and
- validate with experimental results.

2 Experiment

2.1 Material and Specimen

The unidirectional carbon fiber/epoxy IMA/M21 prepreg was obtained from M/s Hexcel in the form of 300 mm wide roll. The nominal thickness of prepreg (lamina) was about 0.18 mm. The prepreg was cut into 300 mm × 450 mm size and laid up on a tool. Teflon sheet of 30 μm thickness was introduced at the mid-thickness (neutral axis) to create an artificial delamination in the test specimens. The composite was then cured in an autoclave maintained at a pressure of 7 bar at 180 °C for 2 h [11]. The vacuum at 1 bar was maintained during curing process. The fiber volume fraction of the fabricated laminate was 59%. The prepared laminates of about 3.8 mm thick were ultrasonically C-scanned. End notched flexure (ENF) test specimen measuring 130 mm × 25 mm was cut from these laminates.

2.2 Spectrum Fatigue Tests

Spectrum fatigue tests were carried out on the ENF specimen in servo-hydraulic test machine under load control mode at an average frequency of 2 Hz (four reversals per second). The photograph of the test setup is shown in Fig. 1a. The schematic, in Fig. 1b, shows the specimen dimensions and the loading arrangement. The fixture is so designed that the specimen can undergo bending either way about the neutral axis and further detailed description about the fixture could be found elsewhere [12]. A standard mini-FALSTAFF load sequence was employed for the spectrum tests. Mini-FALSTAFF is a short version of the FALSTAFF load spectrum [13], which is a standardized variable-amplitude test load sequence developed for the fatigue analysis of materials used for fighter aircraft and is shown in Fig. 2a. One block of this load sequence (N_b = 1) consists of 18,012 reversals at 32 different stress levels and represents loading equivalent of 200 flights. The actual load sequence for experiments and fatigue life prediction was obtained by multiplying all the peak/trough points in the entire block with a reference load. The compliance of the specimen was determined on completion of every load block. Onset-of-growth was assumed, similar to an accepted practice [14, 15] of whenever

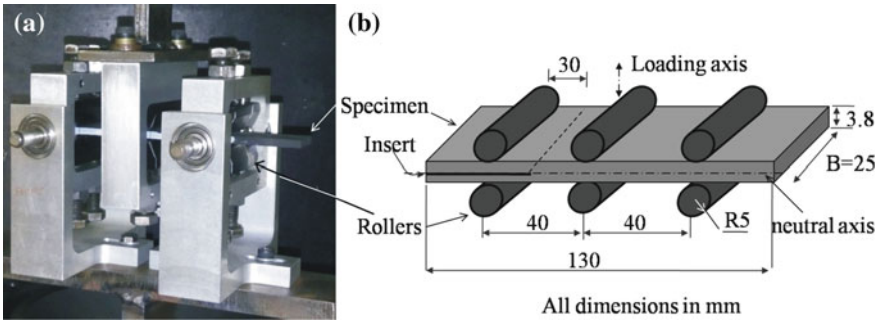

Fig. 1 **a** Photograph of the test setup highlighting the specimen and support rollers; **b** schematic of the test setup

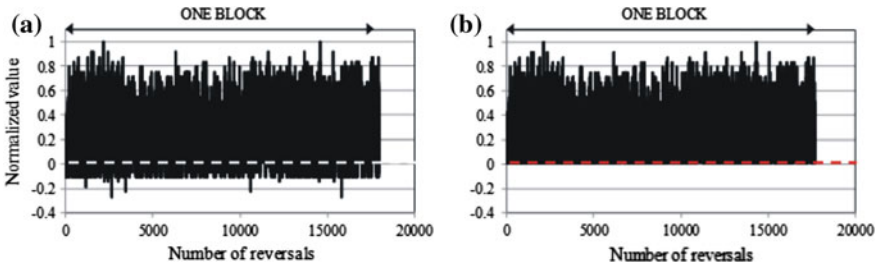

Fig. 2 **a** Mini-FALSTAFF spectrum load sequence; **b** truncated mini-FALSTAFF

5% increase in compliance from the initial value was observed. In our earlier work, a modified form of mini-FALSTAFF, called truncated mini-FALSTAFF, was used wherein all the reversals below zero level were truncated as shown in Fig. 2b [6]. Although the modified mini-FALSTAFF was not used for testing in the present work, the proposed life prediction methodology was tried on the truncated mini-FALSTAFF as well and the results were compared with the results of our earlier work.

2.3 Constant Amplitude Fatigue Tests

As a part of life prediction requirement, constant amplitude (CA) fatigue tests were conducted at three different stress ratios, R = 0.0, 0.5, and −1.0 using a computer controlled 25 kN servo-hydraulic test machine under load control mode, at 2 Hz. The maximum strain energy release rate (maximum SERR or G_{max}) for each of the CA fatigue test was fixed on certain percentage of critical mode II SERR (G_{IIC}) of the material, determined in our earlier work [6]. Measuring the crack tip advance through techniques such as the microscope is extremely difficult and might lead to

erroneous results as the crack remains closed under mode II condition and hence the researchers have suggested the compliance calibration (CC) technique to monitor the crack length [16]. A 5% increase in compliance from the initial value was regarded as N_{onset}.

3 Onset-of-Growth Prediction Methodology

The N_{onset} under the mini-FALSTAFF load sequence was predicted using Palmgren-Miner (PM) empirical method and compared with the experimental results. The methodology employed was similar to the general procedure used for fatigue life prediction for composites under spectrum loads [4]. But the uniqueness in this prediction method lies in the fact that it makes use of only the G_{max}-N_{onset} data (or G-N_{onset}), similar to the S-N data. The flow chart for onset-of-growth prediction is schematically shown in Fig. 3. The procedure of prediction contains:

- Rainflow counting of the fatigue cycles [17] in the spectrum load sequence to obtain individual single cycles with specific G_{max} and G_{min}.

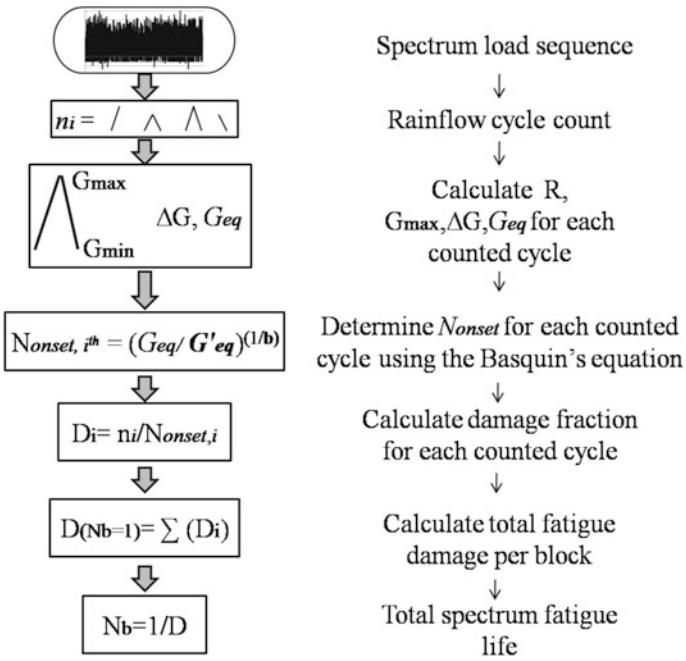

Fig. 3 Flowchart depicting the procedure used for prediction of onset-of-growth under spectrum loading

- Construction of CA G-N_{onset} curves for various stress ratios. Further, the various stress ratio curves are merged using the G_{eq} concept [18] to get the G_{eq}-N_{onset} plot where

$$G_{eq} = \Delta G^{(1-\gamma)} G_{max}^{\gamma} = G_{max}(1-R)^{2(1-\gamma)} \tag{2}$$

and

$$\Delta G = G_{max}(1-R)^2 \tag{3}$$

where γ is the best fit for the G_{eq} curve and will be discussed in subsequent section.
- Determination N_{onset} for each of the counted load cycles using the G_{eq}-N_{onset} plot.
- Calculation of the damage fraction (D_i) for each of the counted load cycles, i, as the ratio of cycle count to $N_{onset,i}$ obtained from the G_{eq}-N_{onset} plot using the Basquin's equation, and, finally,
- Determination of the total fatigue damage per load block (D) by summation of the damage fraction. The material is assumed to fail when the total damage fraction reaches 1.0.

4 Results and Discussion

4.1 *Experimental Onset-of-Growth Under Spectrum Fatigue Tests*

The onset-of-growth behavior of mode II delamination under mini-FALSTAFF load sequence determined experimentally at various reference SERR, G_{Ref} is shown in Fig. 4. Figure 4 also contains the predicted onset-of-growth life which will be

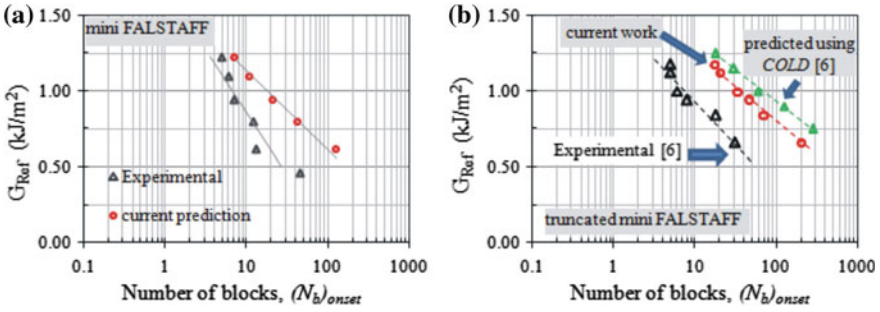

Fig. 4 Experimental and predicted G_{Ref} – $(N_b)_{onset}$ curves for mode II delamination of IMA/M21 CFC determined under, **a** mini-FALSTAFF spectrum load and **b** truncated mini-FALSTAFF

discussed in the subsequent sections. As expected, the onset-of-growth of mode II delamination increased with decrease in reference SERR, G_{Ref}. These results are in similar trend of reference stress-life curves for composites under spectrum loads [19, 20].

4.2 Prediction of Onset-of-Growth Behavior

For the purpose of prediction of onset-of-growth under spectrum loads, the fracture toughness G_{IIC} value was determined (average value is 2.2 kJ/m^2) and the procedure is elaborated in [6]. Following the procedure explained earlier (Fig. 3), the onset-of-growth life was predicted. The predicted number of blocks for onset-of-growth $(N_b)_{onset}$ at various reference SERR (G_{Ref}) under spectrum load sequence is shown along with experimental results in Fig. 4a. Prediction appears to converge with the experimental results at higher G_{Ref} (1.25 kJ/m^2) and drift away as the G_{Ref} decreases. In our earlier work, COLD was used for prediction under modified mini-FALSTAFF load sequence and the prediction was found to be non-conservative (Fig. 4b) [6]. However, it is seen that by making use of proposed methodology (G_{eq}-N_{onset}) the accuracy of prediction may be improved.

4.3 Constant Amplitude Fatigue Tests and Merger of Stress Ratios

The G-N_{onset} curves for IMA/M21 CFC material under mode II condition at three different stress ratios are shown in Fig. 5a. It may be clearly seen that increasing the stress ratio increases the N_{onset}. This is in agreement with similar observations made earlier in polymer composites [21, 22]. The endurance limit also increased with stress ratio, as has been observed by Bak et al. [21]. The experimental G-N_{onset} curves of the IMA/M21 composite were merged into a single curve using the G_{eq} concept, explained in Sect. 3, and fit to an equation similar to Basquin's law as shown in Fig. 5b. A γ value of 0.34 was found to best fit the data points and indicates the relative contribution of ΔG and G_{max}. The Basquin's coefficient (G'_{eq} = 5.37) and exponent (b = −0.24) values were used to estimate N_{onset} and subsequently to calculate the damage fraction per rain flow counted cycle, as explained in Sect. 3. The advantage of having a single R-ratio curve in the G-N_{onset} data is that the subsequent exercise of constructing COLD, used in life prediction models, is overcome and the life prediction is shown to be even better compared to the empirical model tried earlier using COLD data, shown in Fig. 4b.

Delamination studies under static and fatigue loads have been shown to exhibit some significant scatter in test results [23]. The constant amplitude data shown in Fig. 5 also shows a wide scatter. Since this data is fit to an empirical equation and

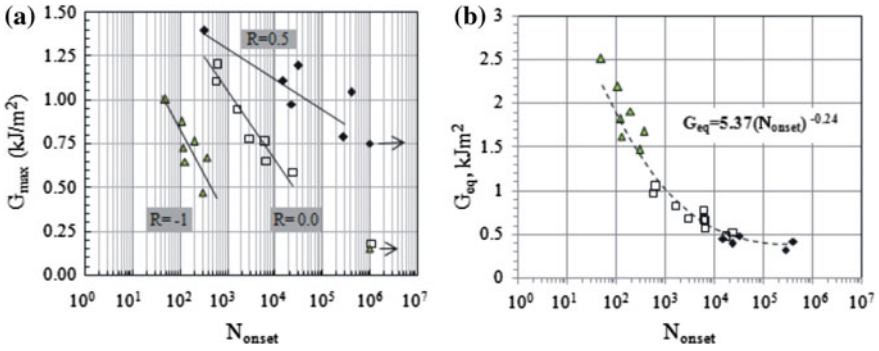

Fig. 5 **a** The constant amplitude G–N_{onset} curves determined for mode II delamination in IMA/M21 CFC material, **b** the three R-ratio curves were merged into a single curve and fit to Basquin's equation

used further in prediction, the scatter may induce errors in predictions. The anomaly in the experimental and the predicted results may be attributed to the scatter in the G-N_{onset} data. Hence, further work would be necessary in understanding the effect of large scatter in the G-N_{onset} data and its effects on prediction.

5 Conclusions

Based on the results obtained from the present investigation, the following conclusions may be drawn:

- The three stress ratio curves of R = 0.5, 0.0, and −1.0 in the G-N_{onset} plot were successfully merged into a single curve using the equivalent SERR (G_{eq}) concept and fit in the form of Basquin's equation. This master plot of G_{eq}-N_{onset} was subsequently used in life prediction methodology
- The predicted results are non-conservative. Nevertheless, further work is required in understanding the effect of large scatter in the G-N_{onset} data on prediction, and possible the use of nonlinear damage accumulation models for onset life prediction.

Acknowledgements Authors wish to thank the AR&DB for financially supporting the project. The support and encouragement provided by Mr. Shyam Chetty, Director, Dr. Satish Chandra, Head, STTD, Dr. Ramesh Sundaram, ACD, CSIR-NAL are acknowledged. Thanks are also due to scientists and technical support staff members of FSIG-STTD and ACD, CSIR-NAL for their assistance in experimental work.

References

1. Hexcel ready to fly on the A350 XWB, Reinf. Plast. **57**, 25–26 (2013)
2. A.C. Garg, Delamination—a damage mode in composite structures. Eng. Frac. Mech. **29**, 557–584 (1988)
3. R.P. Wei, *Fracture Mechanics: Integration of Mechanics, Materials Science, and Chemistry* (Cambridge University Press, 2010)
4. FAA, Composite Aircraft Structure: Advisory Circular (AC) 20-107B, Change 1, FAA (2010)
5. N.L. Post, S.W. Case, J.J. Lesko, Modeling the variable amplitude fatigue of composite materials: a review and evaluation of the state of the art for spectrum loading. Inter. J. Fatigue **30**, 2064–2086 (2008)
6. N. Jagannathan, A.R. Anilchandra, C.M. Manjunatha, Onset-of-growth behavior of mode II delamination in a carbon fiber composite under spectrum fatigue load. Compos. Struct. **132**, 477–483 (2015)
7. M. Wisnom, M. Jones, Through thickness fatigue failure of fibre-reinforced composites. Aeronaut. J. **102**, 83–88 (1998)
8. J. Petermann, A. Plumtree, A unified fatigue failure criterion for unidirectional laminates. Compos. Part A: Appl. Sci. Manuf. **32**, 107–118 (2001)
9. M. Hojo, K. Tanaka, C.G. Gustafson, R. Hayashi, Effect of stress ratio on near-threshold propagation of delamination fatigue cracks in unidirectional CFRP. Compos. Sci. Technol. **29**, 273–292 (1987)
10. I. Maillet, L. Michel, F. Souric, Y. Gourinat, Mode II fatigue delamination growth characterization of a carbon/epoxy laminate at high frequency under vibration loading. Eng. Frac. Mech. **149**, 298–312 (2015)
11. http://www.hexcel.com/Resources/DataSheets/Prepreg-Data-Sheets/M21_global.pdf
12. A.R. Anilchandra, R. Bojja, N. Jagannathan, C.M. Manjunatha, Variable amplitude fatigue testing to characterize mode II delamination in a polymer composite. Trans. Indian Inst. Met. **69**, 421–424 (2016)
13. P. Heuler, H. Klätschke, Generation and use of standardised load spectra and load–time histories. Int. J. Fatigue **27**, 974–990 (2005)
14. W.X. Wang, M. Nakata, Y. Takao, T. Matsubara, Experimental investigation of test methods for mode II interlaminar fracture testing of carbon fiber reinforced composites. Compos. Part A Appl. Sci. Manuf. **40**, 1447–1455 (2009)
15. ASTM D6115, Standard test method for mode I fatigue delamination growth onset of unidirectional fiber-reinforced polymer matrix composites, vol. 15.03. Annual Book of ASTM Standards, ASTM International, West Conshohocken, PA, 2003
16. A.J. Vinciquerra, B.D. Davidson, J.R. Schaff, A.L. Smith, Determination of the mode II fatigue delamination toughness of laminated composites. J. Reinf. Plast. Compos. **21**, 663–677 (2002)
17. ASTM E1049, Standard practices for cycle counting in fatigue analysis. Annual Book of ASTM Standards, ASTM International, West Conshohocken, PA, 2003
18. I. Maillet, L. Michel, F. Souric, Y. Gourinat, Mode II fatigue delamination growth characterization of a carbon/epoxy laminate at high frequency under vibration loading. Eng. Fract. Mech. **149**, 298–312 (2015)
19. C.M. Manjunatha, R. Bojja, N. Jagannathan, Enhanced fatigue performance of a polymer nanocomposite under spectrum loads. Mater. Perform. Charact. **3**, 327–341 (2014)
20. C.M. Manjunatha, R. Bojja, N. Jagannathan, A.J. Kinloch, A.C. Taylor, Enhanced fatigue behavior of a glass fiber reinforced hybrid particles modified epoxy nanocomposite under WISPERX spectrum load sequence. Int. J. Fatigue **54**, 25–31 (2013)

21. B.L.V. Bak, C. Sarrado, A. Turon, J. Costa, Delamination under fatigue loads in composite laminates: A review on the observed phenomenology and computational methods. Appl. Mech. Rev. **66**, 1–24 (2014)
22. A. Argüelles, J. Viña, A.F. Canteli, M.A. Castrillo, J. Bonhomme, Interlaminar crack initiation and growth rate in a carbon-fibre epoxy composite under mode-I fatigue loading. Compos. Sci. Technol. **68**, 2325–2331 (2008)
23. T.K. O'Brien, W.M. Johnston, G.J. Toland, Mode II interlaminar fracture toughness and fatigue characterization of a graphite Epoxy Compos Mater, NASA/TM–2010-216838